

Polygonal Chains Cannot Lock in 4D

Roxana Cocan and Joseph O'Rourke*

November 9, 2018

Abstract

We prove that, for all dimensions $d \geq 4$, every simple open polygonal chain may be straightened, and every simple closed polygonal chain may be convexified. Both can be achieved by algorithms that use polynomial time in the number of vertices, and result in a polynomial number of “moves.” These results contrast to those known for $d = 3$, where open and closed chains can be “locked.”

Smith Technical Report 063

Full version of abstract in

Proceedings of the 11th Canadian Conference on Computational Geometry
Vancouver, August 1999.

*Dept. of Computer Science, Smith College, Northampton, MA 01063, USA. {rcocan, orourke}@cs.smith.edu. Research supported by NSF Grant CCR-9731804. This is a minor revision of the June 16, 1999, Technical Report of the same number.

Contents

1	Introduction	1
1.1	Summary	1
1.2	Background	2
2	Straightening Open Chains in 4D	3
2.1	Algorithm 1a	3
2.1.1	2: s_g is free	4
2.1.2	1: s_g is intersected	6
2.1.3	Motion Planning	8
2.2	Algorithm 1b	8
2.2.1	3: w is free	10
2.2.2	2: w is obstructed (but s_g is not intersected)	10
2.2.3	Algorithm 1b Complexity	12
2.3	Implementation	12
3	Convexifying Closed Chains in 4D	12
3.1	Choosing L	14
3.2	Line Tracking in 3D	16
3.2.1	Topology of Configuration Space in 3D	16
3.2.2	Obstruction Diagram in 3D	16
3.2.3	Disconnected Free Space in 3D	18
3.3	Line Tracking in 4D	18
3.3.1	Topology of Configuration Space in 4D	19
3.3.2	Obstruction Diagram in 4D	19
3.3.3	Connected Free Space in 4D	22
3.4	Motion Planning	25
4	Higher Dimensions	25

1 Introduction

1.1 Summary

A *polygonal chain* $P = (v_0, v_1, \dots, v_n)$ is a sequence of consecutively joined segments $s_i = v_i v_{i+1}$ of fixed lengths $\ell_i = |s_i|$, embedded in space. A chain is *closed* if the line segments are joined in cyclic fashion, i.e., if $v_n = v_0$; otherwise, it is *open*. A chain is *simple* if only adjacent edges intersect, and only then at the endpoint they share. We study reconfigurations of simple polygonal chains, continuous motions that preserve the lengths of all edges while maintaining simplicity throughout. One basic goal is to determine if an open chain can be *straightened*—stretched out in a straight line, and whether a closed chain can be *convexified*—reconfigured to a planar convex polygon. If neither is possible, the chain is called *locked*. This terminology is borrowed from [BDD⁺99].

It is an open problem to determine if every open (or closed) chain in 2D can be straightened (or convexified). See [ELR⁺98] for partial results. In 3D it is known that there exist both open and closed chains that are locked [CJ98, BDD⁺99, Tou99], and several special cases are known to be unlocked [BDD⁺99]. In this paper we prove that, for all dimensions $d \geq 4$, neither open nor closed chains can lock. We partition our results into three main theorems:

Theorem 1 *Every simple open chain in 4D may be straightened, by an algorithm that runs in $O(n^3 \alpha(n))$ time and $O(n^2)$ space, and which accomplishes the straightening in $O(n)$ moves.*

Here “move” is used in the sense defined in [BDD⁺99].¹ Essentially each move is a simple monotonic rotation of a few joints. The term $\alpha(n)$ is the nearly constant inverse of Ackermann’s function. We have implemented this algorithm for the case when the vertices are in general position, when it is straightforward.

Theorem 2 *Every simple closed chain in 4D may be convexified, by an algorithm that runs in $O(n^6 \log n)$ time, and which accomplishes the straightening in $O(n^6)$ moves.*

Theorem 3 *Both Theorems 1 and 2 hold for all dimensions $d \geq 4$, i.e., polygonal chains cannot lock in dimensions greater than three.*

We partition the results this way because the proofs of these three theorems are rather different. In particular, the proof of Theorem 3 is not difficult.

We summarize our results in the context of earlier work in the table below.

Dimension	(Un)Locked
2	?
3	\exists locked chains
$d \geq 4$	Cannot lock

¹ “During each move, a (small) constant number of individual joint moves occur, where for each a vertex v_{i+1} rotates monotonically about an axis through joint v_i , with the axis of rotation fixed in a reference frame attached to some edges.”

1.2 Background

Before commencing with our technical arguments, we start with some background, with the intent of providing intuition to support our results.

No Knots in 4D. In [CJ98] and [BDD⁺99], the same example of a locked open chain in 3D is provided. The version in the latter paper is shown in Fig. 1.

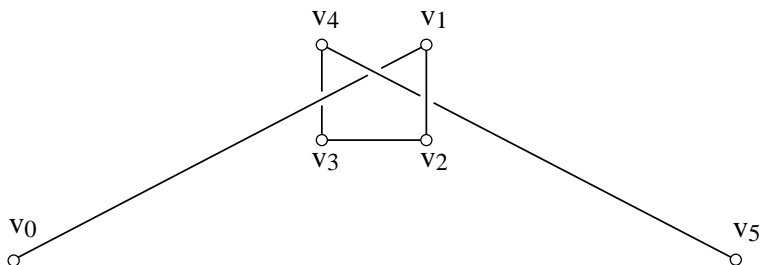


Figure 1: The “knitting needles” example, based on Fig. 1 in [BDD⁺99] (by permission).

One proof (used in [BDD⁺99]) that this chain K is locked depends on closing the chain by connecting v_0 to v_5 to form K' , and then arguing that K can be straightened iff the corresponding trefoil knot K' can be unknotted, which of course it cannot. Thus there is a close connection in 3D between locked chains and knots. However, the following theorem is well known:

Theorem 4 *No 1D closed, tame,² nonself-intersecting curve C is knotted in \mathbb{R}^4 .*

See, e.g., [Ada94, pp.270-1] for an informal proof. Because proofs of this theorem employ topological deformations, it seems they are not easily modified to help settle our questions about chains in 4D. The rigidity of the links prevents any easy translation of the knot proof technique to polygonal chains. However, it does suggest that it would be difficult to construct a locked chain by extending the methods used in 3D.

No Cages in 4D. A second consideration lends support to the intuition behind our main claim. This is the inability to confine one segment in a “cage” composed of other segments in 4D. Consider segment $s_0 = v_0v_1$ in Fig. 1. It is surrounded by other segments in the sense that it cannot be rotated freely about one endpoint (say v_0) without colliding with the other segments. Let S^2 be the 2-sphere in \mathbb{R}^3 of radius ℓ_0 centered on v_0 . Each point on S^2 is a possible location for v_1 . Segment s_0 is confined in the sense that there are points of S^2

² A curve is *tame* if it is topologically equivalent to a polygonal curve [CF65, p.5]. Any curve that is continuously differentiable, i.e., in class C^1 , is tame.

that cannot be reached from s_0 's initial position without collision with the other segments. This can be seen by centrally projecting the segments from v_0 onto S^2 , producing an “obstruction diagram.” It should be clear that v_1 is confined to a cell of this diagram. Although this by no means implies that the chain in Fig. 1 is locked, it is at least part of the reason that the chain might be locked.

We now argue informally that such confinement is not possible in 4D. Again let $s_0 = v_0v_1$ be fixed at v_0 , and let S^3 be the 3-sphere in \mathbb{R}^4 of radius ℓ_0 centered on v_0 that represents the possible locations for v_1 . Again we project the other segments onto S^3 producing an obstruction diagram. As in the lower dimensional case, this diagram is composed of 1D curves, being the projection of 1D segments. On the surface of S^2 , these curves can confine v_1 . But in S^3 , which is a 3D space, no (finite) set of 1D curves can confine v_1 , which has three degrees of freedom. Our next task is to make this intuitive argument more precise.

2 Straightening Open Chains in 4D

Let P be a simple, open polygonal chain in 4D with $n \geq 2$ vertices. Each vertex v_i is also called a *joint* of the chain. The segment $s_i = v_iv_{i+1}$ we sometimes call a *link* of the chain. We say a joint v_i is *straightened* if (v_{i-1}, v_i, v_{i+1}) are collinear and form a simple chain; in this case, the angle at v_i is π .

We prove Theorem 1 by straightening the first joint v_1 , “freezing” it, and repeating the process until the entire chain has been straightened. This is a procedure which, of course, could not be carried out in 3D. But there is much more room for maneuvering in 4D. We have two different algorithms for accomplishing this task. The first (Algorithm 1a) is easier to understand, but only establishes a bound of $O(n^4)$ on the number of moves, and requires $O(n^4 \log n)$ time. The second (Algorithm 1b) is a bit more intricate but achieves $O(n)$ moves in nearly cubic time. Both follow the rough outline just sketched. We provide full details for Algorithm 1a, but only sketch Algorithm 1b.

Define the *goal position* v_g for v_0 (and $s_g = v_gv_1$ the goal position for s_0) as the unique position that represents straightening of joint v_1 . Call the goal position *intersected* if $s_g \cap s_i \neq \emptyset$ for some $i > 2$; and otherwise call it *free*.

2.1 Algorithm 1a

A high-level view of the algorithm is as follows:

Algorithm 1a: Open Chains

repeat until chain straightened do

1: if s_g is *intersected* thenConstruct obstruction diagram $\text{Ob}(v_1)$ on S^2 .Move v_1 so that the goal position is not intersected.2: else s_g is *free*Construct obstruction diagram $\text{Ob}(v_0)$ in S^3 .Apply motion planning to move v_0 to v_g .

We consider the two numbered steps in reverse order.

2.1.1 2: s_g is free

Our argument depends on some basic intersection facts, which we formulate in \mathbb{R}^d in a series of lemmas before specializing to the $d = 3$ and $d = 4$ cases we need.

Geometric Intersections in \mathbb{R}^d . Let the coordinates of \mathbb{R}^d be x_1, x_2, \dots, x_d ; when convenient we will use x, y, z for the first three coordinates. A kD *flat* is a k -dimensional affine subspace of \mathbb{R}^d , i.e., a subspace spanned by k vectors, not necessarily containing the origin. Flats for $k = 0, 1, 2$ are also called points, lines, and planes. A k -sphere is a sphere whose surface is k -dimensional. A circle is a 1-sphere, and a sphere in \mathbb{R}^3 is a 2-sphere.

Lemma 1 *The intersection of a 2D plane π with a $(d-1)$ -sphere S in \mathbb{R}^d is a circle, a point, or empty.*

Proof: Translate and rotate the sphere and plane so that the sphere is centered on the origin, and the plane is parallel to the x_1x_2 -plane. The equations of the sphere S and the plane π are then:

$$S : x_1^2 + x_2^2 + \dots + x_d^2 = r^2 \quad (1)$$

$$\pi : x_3 = a_3, x_4 = a_4, \dots, x_d = a_d \quad (2)$$

where the a_i are constants. Let $A^2 = \sum_{i=3}^d a_i^2$. Then

$$S \cap \pi : x_1^2 + x_2^2 + A^2 = r^2 \quad (3)$$

$$x_1^2 + x_2^2 = r^2 - A^2 \quad (4)$$

If $r^2 < A^2$, the intersection is empty. If $r^2 = A^2$, the intersection is the point $(0, 0, a_3, \dots, a_d)$. If $r^2 > A^2$, the intersection is a circle in π with radius $\sqrt{r^2 - A^2}$, and center $(0, 0, a_3, \dots, a_d)$. \square

Lemma 2 *The intersection of a (1D) line, ray, or segment with a $(d-1)$ -sphere S in \mathbb{R}^d is at most two points, i.e., either two points, one point, or empty.*

Proof: Let $s = ab$ be a segment, and let the sphere center be c . Let π be the 2D plane determined by the three points a, b, c , i.e., π is the affine span of $\{a, b, c\}$. Because $s \subset \pi$, we must have $s = s \cap \pi$. So

$$s \cap S = (s \cap \pi) \cap S \tag{5}$$

$$= s \cap (\pi \cap S) \tag{6}$$

By Lemma 1, $\pi \cap S$ is a circle, and the claim for segments follows because a segment intersects a circle in at most two points. Rays and lines yield the same result by selecting a and b sufficiently large. \square

Let $\Delta = (a, b, c)$ be a triangle in \mathbb{R}^d . We call the set of points that lie on rays that start at c and pass through a point of ab a (2D) *triangle cone* $\Delta_c(a, b)$. If (a, b, c) are collinear, the triangle degenerates to a segment, and the triangle cone degenerates to a line or ray.

Lemma 3 *The intersection of a (2D) triangle $\Delta(a, b, c)$ or triangle cone $\Delta_c(a, b)$ with a $(d-1)$ -sphere S in \mathbb{R}^d , whose center is at c , consists of at most two arcs of a circle, i.e., it is a set of at most two connected components, each of which is either an arc of a circle or a point.*

Proof: Let π be the 2D plane containing Δ . Because $\Delta \subset \pi$, $\Delta = \Delta \cap \pi$. So $\Delta \cap S = \Delta \cap (\pi \cap S)$. By Lemma 1, $\pi \cap S$ is a circle C in the plane containing Δ ; it is clear that c is the center of this circle. The result follows from the possible intersections between a triangle or triangle cone, with apex at c , with a circle centered on c . \square

Obstruction Diagram $\text{Ob}(v_0)$. Let \mathcal{C}_0 be the *configuration space* for vertex v_0 when v_1 is fixed: the set of all possible positions for v_0 that preserve the length of $v_1 v_0$. \mathcal{C}_0 is a 3-sphere S^3 in \mathbb{R}^4 centered on v_1 with radius ℓ_0 .³ It is a 3D manifold⁴ with the topology S^3 . Let \mathcal{F}_0 be the *free space* for vertex v_0 with all other vertices v_i of the chain fixed: the subset of \mathcal{C}_0 for which the chain is simple, i.e., for which s_0 does not intersect s_i , $i > 1$. We define the *obstruction diagram* $\text{Ob}(v_0)$ for v_0 as the set such that $\mathcal{F}_0 = \mathcal{C}_0 - \text{Ob}(v_0)$. Our goal is to describe, and ultimately construct, $\text{Ob}(v_0)$.

Let V_i be the set of points of S that represent positions of $s_0 = v_0 v_1$ that intersect segment s_i . Thus $\text{Ob}(v_0) = \bigcup_{i=2}^n V_i$.

Lemma 4 *The set of points $V_i \subset S^3$ consists of at most two arcs of a circle, where S^3 and V_i are defined as above.*

Proof: Let $\Delta = \Delta_{v_1}(v_i, v_{i+1})$ be the triangle cone of rays from v_1 through a point of $s_i = v_i v_{i+1}$. Clearly if s_0 intersects s_i , s_0 lies in this cone. Thus Δ is a superset of all the points on s_0 when it intersects s_i . Because S^3 is the set of v_0 endpoint positions of s_0 , $V_i = \Delta \cap S^3$. The claim then follows from Lemma 3. \square

Lemma 5 *The set of points $\text{Ob}(v_0) \subset S^3$ consists of at most $2(n-1)$ arcs of a circle.*

³ The superscript on S is to remind us of the dimensionality of the sphere.

⁴ See [Thu97, p. 33] for an intuitive description of this manifold.

Proof: Follows immediately from $n-1$ applications of Lemma 4. \square

This lemma is now immediate:

Lemma 6 *If v_0 's goal position v_g is free, then v_1 may be straightened.*

Proof: Because v_g is free, $v_g \notin \text{Ob}(v_0)$. Because the given chain is assumed simple, the initial position $v_0 \notin \text{Ob}(v_0)$. The space S^3 of possible positions of v_0 is a 3D manifold, a 3-sphere. The obstacles $\text{Ob}(v_0)$ are a finite set of 1D circle arcs and points. The removal of $\text{Ob}(v_0)$ from S^3 cannot disconnect v_0 from v_g .⁵ Therefore there is a path in $\mathcal{F}_0 = S^3 \setminus \text{Ob}(v_0)$ from v_0 to v_g , which represents a continuous motion of s_0 that straightens v_1 . \square

It is this lemma which justifies the claim made in Section 1.2 that there can be no cages in 4D. We will defer to Section 2.1.3 construction of the path guaranteed by this lemma.

2.1.2 1: s_g is intersected

If s_g is intersected, then rotating s_0 to the goal position necessarily violates simplicity at the goal position. In this case, we move v_1 , the joint between s_0 and s_1 , so that the new goal position s'_g is no longer intersected.

We will need a slight strengthening of Lemma 3, which does not require that the triangle's apex be at the sphere center:

Lemma 7 *The intersection of a (2D) triangle $\Delta(a, b, c)$ or triangle cone $\Delta_c(a, b)$ with a $(d-1)$ -sphere S in \mathbb{R}^d , is a set of at most three connected components, each of which is either a circle, an arc of a circle, or a point.*

Proof: As before, we may restrict attention to the intersection of the 2D plane π containing the triangle or triangle cone. Lemma 1 then reduces the problem to intersecting a triangle and a circle, and the claim follows. See Fig. 2. \square

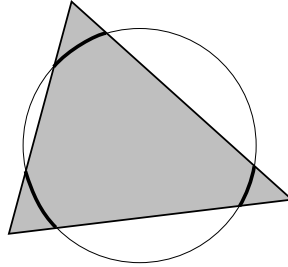


Figure 2: The intersection of a triangle and a sphere is at most three arcs.

That we can “break” the degeneracy of an intersected goal is established by this lemma:

⁵ “ \mathbb{E}^d cannot be separated by a subset of dimension $\leq d-2$.” [HY61, p. 148].

Lemma 8 v_1 may be moved to v'_1 while keeping all other vertices fixed, so that the chain remains simple, and the new goal s'_g is not intersected. The move may be computed in $O(n^2\alpha(n))$ time and $O(n^2)$ space.

Proof: Fix the positions of $v_0, v_2, v_3, \dots, v_n$. The sphere

$$S^2 = \{z \in \mathbb{R}^4 : |z - v_0| = \ell_0, |z - v_2| = \ell_1\}$$

represents all the possible positions for v_1 that preserve the lengths of its incident links. S^2 has the topology \mathbb{S}^2 . That it is a 2-sphere can be seen by analogy with the lower-dimensional situation. For if the chain were in 3D, v_1 would lie on the intersection of two 2-spheres, centered at v_0 and v_2 , and so would (in nondegenerate cases) be a 1-sphere, a circle. Similarly in 4D, v_1 lies on the intersection of two 3-spheres, and so is a 2-sphere. Because we may assume that v_1 is not already straightened, S^2 does not degenerate to a point.

Now we construct an obstruction diagram $\text{Ob}(v_1)$ on S^2 representing all those positions of v_1 for which the goal position s_g is intersected, or for which the chain (v_0, v_1, v_2) intersects the remaining, fixed chain (v_2, \dots, v_n) . We first concentrate on intersected goal positions s_g .

Such an s_g is contained in the ray from v_2 through $v_1 \in \text{Ob}(v_1)$. Let ${}_2\Delta_i$ be the triangle cone with apex at v_2 and delimited by s_i : ${}_2\Delta_i = \Delta_{v_2}(v_i, v_{i+1})$. Clearly any intersected s_g is contained in some Δ_i for $i > 2$. See Fig. 3. Thus

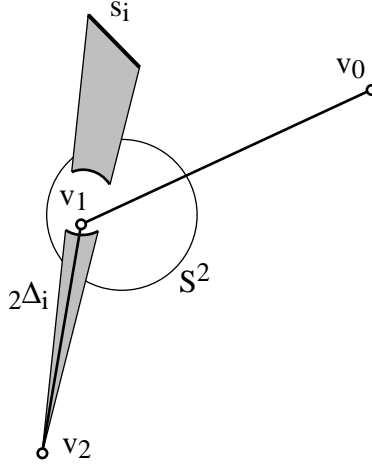


Figure 3: The triangle cone ${}_2\Delta_i$ intersects the sphere S^2 in some circle arcs.

the intersection of ${}_2\Delta_i \cap S^2$ is a superset of the positions forbidden for v_1 due to intersected goal positions. (The reason it is a superset is that it may be that s_g does not reach s_i , although it would were ℓ_0 longer.)

$\text{Ob}(v_1)$ also contains all the positions of v_1 that cause the two adjacent links to intersect any of the other segments. The link v_2v_1 is clearly covered by ${}_2\Delta_i$.

The link v_0v_1 can be handled by the analogous triangle cone ${}_0\Delta_i$ with apex at v_0 and through s_i : ${}_0\Delta_i = \Delta_{v_0}(v_i, v_{i+1})$. Let $\Delta_i = {}_0\Delta_i \cup {}_2\Delta_i$.

By Lemma 7, the Δ_i , $i > 1$, intersect S^2 in a finite number of circles, arcs, and points (at most $2 \cdot 3(n-2) = O(n)$). Thus $\text{Ob}(v_1)$ is contained in a such a set V .

We now construct this V as an arrangement of circular arcs on a sphere. This can be accomplished in $O(n^2\alpha(n))$ time and $O(n^2)$ space [EGP⁺92, Hal97]. By hypothesis, the original s_g is intersected, which means that $v_1 \in \text{Ob}(v_1) \subset V$. Let $Z = \{a_1, \dots, a_m\}$ be the collection of arcs of V that contain v_1 . Z may be found by a brute force check of each of the $O(n)$ arcs.

Compute the minimum distance α on S^2 from v_1 to arcs not in Z : to those in $V \setminus Z$. Then the spherical disk U of radius $\alpha/2$ centered on v_1 is a neighborhood of v_1 that has no points in common with arcs not in Z . Any point in $U \setminus Z$ can serve as v'_1 . To be specific, we could bisect the angle between two arcs of Z angularly consecutive around v_1 , and move off $\alpha/2$ along that direction.

Moving (in one move) v_1 to v'_1 establishes a new goal s'_g that is not intersected.⁶ \square

2.1.3 Motion Planning

Now that we know we can perform Step 1 of Algorithm 1a in time $O(n^2\alpha(n))$ per iteration, we return to finding a path through S^3 for v_0 , as guaranteed by Lemma 6. Motion planning between two points of $\mathcal{F} = S^3$ in the same connected component may be achieved by any general motion planning algorithm [Sha97, Sec. 40.1.1]. For example, Canny's Roadmap algorithm achieves a time and space complexity of $O(n^k \log n)$, where n is the number of obstacles, and k the number of degrees of freedom in the robot's placements. In our case, $k = 3$. His algorithm produces a piecewise algebraic path through \mathcal{F} , of $O(n^k)$ pieces. Each piece constitutes a constant number of moves, with the constant depending on the algebraic degree of the curves, which is bounded as a function of k . Therefore each joint straightening can be accomplished in $O(n^3)$ moves. Repeating the planning and straightening n times leads to $O(n^4)$ moves in $O(n^4 \log n)$ time. In the next section we reduce the $O(n^3)$ moves per joint straightening to just 3 moves per straightening.

2.2 Algorithm 1b

We have now established Theorem 1, but with weaker complexity bounds than claimed. It is not surprising that applying a general motion planning algorithm is wasteful in our relatively simple situation. And in fact a significant improvement over Algorithm 1a can be achieved by switching attention from the absolute position of v_0 , to the direction in which s_0 rotates. Let the vector along s_0 be $w_0 = v_0 - v_1$, and similarly let $w_g = v_g - v_1$. Let w be the *goal*

⁶ Note that it is quite possible for v_1 to be confined within a cell of the arrangement $\text{Ob}(v_1)$, but that this "cage" is no impediment. For we do not need a path from v_1 to an arbitrary point of S^2 ; rather we only need a path to any unobstructed point v'_1 .

direction: a unit vector orthogonal to w_g that represents the direction in which w_0 should be rotated to move it to its goal position. See Fig. 4. Thus w is the

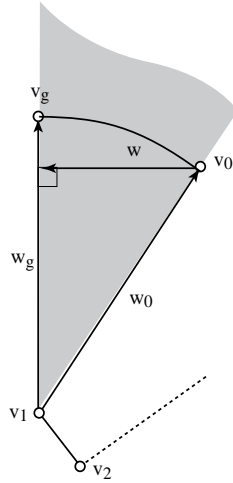


Figure 4: The goal direction vector w defines the direction that w_0 should be rotated to reach w_g . The shaded cone is not crossed by an links of the chain if w is unobstructed.

unique vector orthogonal to w_g such that

$$a_1 w_g + b_1 w = w_g - w_0 \quad (7)$$

for some reals $a_1 > 0$ and $b_1 > 0$: i.e., it is difference vector $w_g - w_0$ expressed in the basis (w_g, w) . The space of possible directions w is \mathbb{S}^2 rather than the \mathbb{S}^3 we faced in Step 1 of Algorithm 1a. This permits replacing the $O(n^3)$ moves per step from motion planning, to at most two moves. We now proceed to describe this. In the interest of brevity, some of the proofs are not fully formalized. More detailed proofs are contained in [Coc99].

Algorithm 1b distinguishes three possibilities:

1. The goal position is *intersected* by some other link of the chain (just as in Algorithm 1a).
2. The goal direction is *obstructed* in that rotation of s_0 in the direction w might hit some link of the chain along its direct rotation to the goal position.
3. The goal direction is *free*: it is not obstructed (and so the goal position is not intersected).

A high-level view of our second algorithm is as follows:

Algorithm 1b: Open Chains
repeat until chain straightened do
1: if s_g is *intersected* then
Move v_1 so that the goal position is not intersected.
2: else if w is *obstructed* then
Rotate s_0 to new position whose goal direction is free.
3: else if w is *free* then
Rotate s_0 directly to s_g .

Step 1 is identical to that employed in Algorithm 1a. We discuss the other two steps in reverse order.

2.2.1 3: w is free

By our definitions, s_0 may be rotated directly to s_g without hitting any other segment of the chain. Because the goal position s_g is not intersected, the chain remains simple even after the rotation has been completed. Therefore, the link s_0 can be straightened in one move.

Note that this is the generic situation, in that for a “random” chain, e.g., one whose vertex coordinates are chosen randomly from a 4D box, each link can be straightened with Step 3 of the algorithm with high probability. Steps 1 and 2 handle “degenerate” cases. We exploit this in our implementation (Section 2.3).

2.2.2 2: w is obstructed (but s_g is not intersected)

Detecting obstructions. When w is obstructed, we again rely on construction of an obstruction diagram. First we describe the space in which the obstruction diagram is embedded.

Consider the space of possible directions from which s_0 might approach s_g . In 3D, this set of unit vectors forms a circle \mathbb{S}^1 , which can be viewed as orthogonal to s_g and centered on v_g ; see Fig. 5a. Similarly, in 4D, the set of possible approach directions toward s_g forms a 2-sphere \mathbb{S}^2 , which we center on v_g . Every point on this sphere represents a direction of approach to s_g ; see Fig. 5b. Note we consider approach directions to s_g rather than departure directions from s_0 , because the former is fixed on the unmoving s_g , whereas we will be moving s_0 .

The *obstruction diagram* $\text{Ob}(s_g)$ is the set of vectors w representing obstructed goal directions for s_g .

Lemma 9 *If the goal s_g is not intersected, the obstruction diagram $\text{Ob}(s_g)$ consists of at most $2n$ arcs on \mathbb{S}^2 .*

Proof: Take an arbitrary segment s_i of the chain, and project it into the 3D subspace containing the sphere \mathbb{S}^2 representing all unit directions w orthogonal to s_g . s'_i is the intersection of the cone $C_{v_1}(s_i)$ with Π , the 3D subspace orthogonal to s_g and containing v_g . We first claim that the set of directions w obstructed by s'_i is identical to those obstructed by s_i .

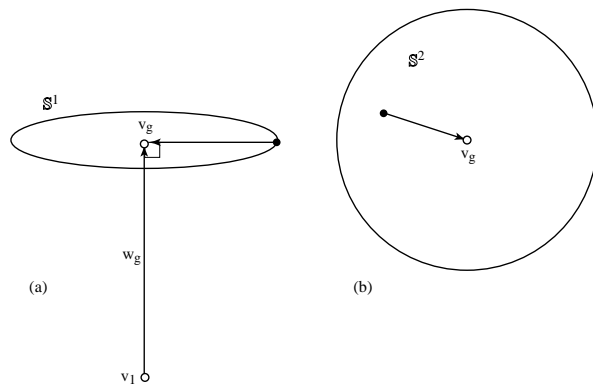


Figure 5: (a) Directions approaching the goal position in 3D; (b) in 4D.

Now every vector w determined by a point on \mathbb{S}^2 and its center v_g is orthogonal to s_g by our choice of Π . So the set of w obstructed by s'_i is just those w determined by the intersection of $C_{v_g}(s'_i)$ with \mathbb{S}^2 , and is therefore at most two arcs on the sphere. See Fig. 6.

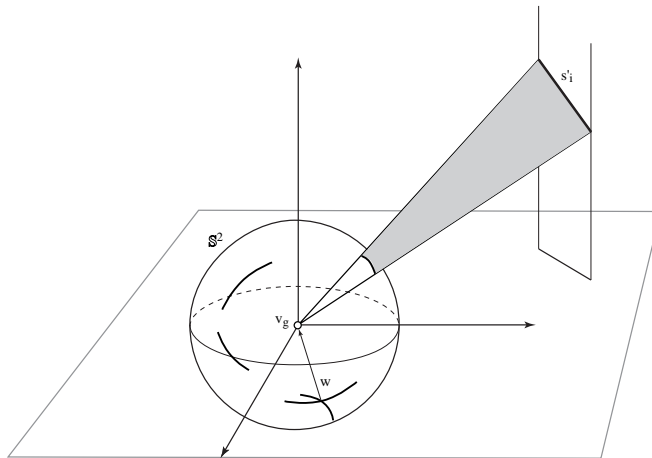


Figure 6: In 4D, s_i projects to s'_i in the 3D subspace containing \mathbb{S}^2 , and produces an arc of the obstruction diagram determined by the intersection of the triangle (v_g, s'_i) with \mathbb{S}^2 .

Because we assumed that the goal is not intersected, we know s_i does not lie along the line containing s_g , and therefore s'_i does not include the center of the sphere v_g . Thus the obstruction arc for one segment has length $< \pi$. \square

Lemma 10 *The obstruction diagram $Ob(s_g)$ may be constructed in $O(n^2\alpha(n))$*

time and $O(n^2)$ space, and used to detect whether or not w is obstructed. \square

Skirting obstructions. If w is obstructed, then w touches one or more arcs of the obstruction diagram, as illustrated in Fig. 6. Our next task is to move s_0 when w is obstructed so that its new goal direction is free. It is relatively easy to find a Δw that will move w to be free:

Lemma 11 *If w is obstructed, s_0 can be moved so that its new goal direction $w' = w + \Delta w$ is unobstructed. Δw may be computed in $O(n)$ time from $Ob(s_g)$.*

Proof: The proof of this lemma is nearly identical to that of Lemma 8, and will not be presented. \square

Note that because we have based our analysis on a fixed s_g , moving s_0 does not alter the obstruction diagram, which records obstructed directions of approach to s_g .

2.2.3 Algorithm 1b Complexity

The algorithm straightens one joint in at most three moves: one to move v_1 so the goal is not intersected (Step 1), one to move v_0 so that the goal is not obstructed (Step 2), and one to rotate directly to the goal (Step 3). The total number of moves used by the algorithm is then most $3n = O(n)$. For each of the n iterations, the relevant obstruction diagrams can be constructed in $O(n^2\alpha(n))$ time and $O(n^2)$ space. This then establishes the total time complexity of $O(n^3\alpha(n))$ claimed in Theorem 1. Because each move is performed independently, the obstruction diagrams may be discarded after each iteration. Thus the space requirements remain at $O(n^2)$.

2.3 Implementation

We have implemented Algorithm 1b for chains in “general position” in C++. The program accepts a chain as input, and first checks if it is simple. If it is, the straightening process starts; otherwise the program exits. The program then straightens the chain link by link using Step 3. It also detects whether the goal is obstructed or intersected, but in those cases it again simply halts; we have not implemented the obstruction diagrams. For a chain whose vertex coordinates are chosen randomly, the program straightens it with high probability, for then the degenerate cases handled by Steps 2 and 3 of the algorithm are unlikely to occur. The output of the program is a set of Geomview files that animate the straightening process. See Fig. 7 for an example.

3 Convexifying Closed Chains in 4D

Our algorithm for convexifying closed chains employs the *line tracking* motions introduced in [LW95]. Indeed our algorithm mimics theirs in that we repeatedly

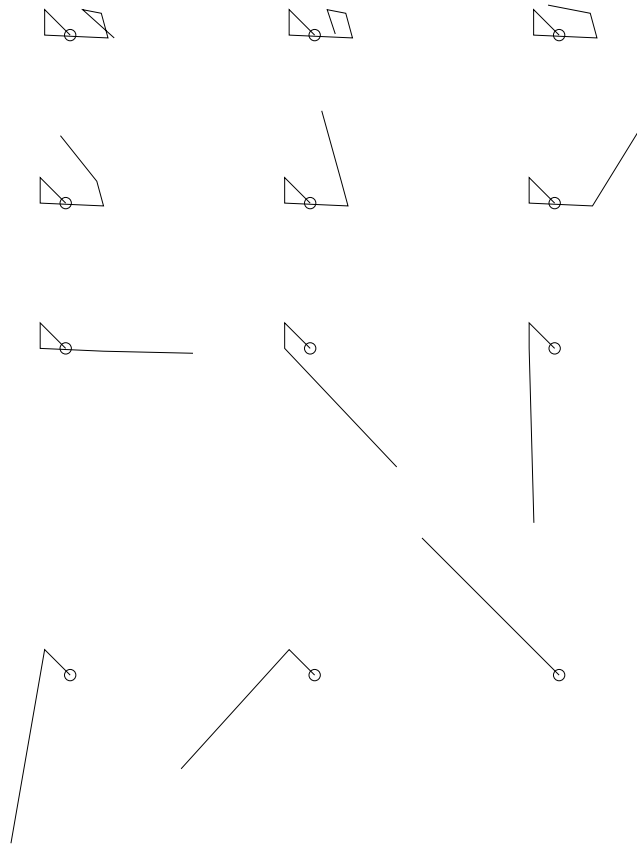


Figure 7: Snapshots of the algorithm straightening a chain of 6 links. Time advances left to right, top to bottom. The last vertex v_n , which never moves, is circled in each chain. The apparent link length changes are an artifact of the orthographic projection of the 4D chain down to 2D.

apply line tracking motions, each of which straightens at least one joint, until a triangle is obtained (which is a planar convex polygon, as desired). Although the overall design of our algorithm is identical, the details are quite different, for there is a major differences with [LW95]: They permitted self-intersections of the chain, whereas we do not. This greatly complicates our task.⁷

Let $(v_0, v_1, v_2, v_3, v_4)$ be five consecutive vertices of a closed polygonal chain. We allow $v_0 = v_4$. A *line tracking* motion of v_2 moves v_2 along some line L in space, while keeping both v_0 and v_4 fixed. As long as the angle at joints v_1 and v_3 (the *elbows*) are neither π (straight) nor 0 (folded), such a motion is possible. Neither angle can be 0 because that would violate the simplicity of the chain. Straightening one joint is precisely our goal, so we assume that neither joint is straight; and therefore a line tracking motion is possible.

We will choose L and a direction along it so that the movement increases the distance from v_2 to both v_0 and v_4 simultaneously. This necessarily opens both elbow angles. The motion stops when one elbow straightens. The only issue is whether this can be done while maintaining simplicity. Our aim is to prove this theorem:

Theorem 5 *For a simple 4D chain (v_0, \dots, v_4) , there exists a line tracking motion of v_2 that straightens either v_1 or v_3 (or both) while maintaining simplicity of the chain throughout the motion.*

A high-level view of the algorithm is as follows:

Algorithm 2: Closed Chains
repeat until chain is a triangle do
 Compute a line L along which to move v_2 .
 Compute free paths π_1 and π_3 for v_1 and v_3 .
 Move v_2 along L , v_1 along π_1 , and v_3 along π_3 .
 Freeze the straightened joint v_1 or v_3 .

3.1 Choosing L

To fix L , the ray along which v_2 moves, we choose a point $q \in \mathbb{R}^4$ different from v_2 , and let L be the ray from v_2 that contains v_2q . We will choose q so that it is itself the point where one of the two joints v_1 or v_3 becomes straight while moving v_2 along L .

Lemma 12 *A point q determining an appropriate L may always be found, and in time and space $O(n^4)$.*

Proof: We choose q so that it satisfies these conditions:

1. Moving v_2 along L increases the distance from v_2 to v_0 and from v_2 to v_4 .

⁷ An alternative convexifying algorithm, again permitting self-intersections, is described in [Sal73]. Sallee accomplishes the same result by a different basic motion, involving four consecutive vertices rather than the five used in [LW95].

2. $|qv_0| = |v_0v_1| + |v_1v_2| = r_0$, or $|qv_4| = |v_2v_3| + |v_3v_4| = r_4$ (i.e., either v_1 or v_3 becomes straight).
3. (a) If $|qv_0| = |v_0v_1| + |v_1v_2| = r_0$, then qv_0 does not intersect any other segment of the chain than those to which it is incident.
- (b) If $|qv_4| = |v_2v_3| + |v_3v_4| = r_4$, then qv_4 does not intersect any other segment of the chain than those to which it is incident.

Condition 3 ensures that our “goal” is not itself intersected, in the sense used in Section 2.

Let S_i be the set of points of \mathbb{R}^4 that satisfy Condition i above. S_1 is the intersection of two closed half-spaces containing v_2 , orthogonal to v_0v_2 and v_2v_4 respectively. Note that $v_2 \in S_1$. If v_0v_4 and v_2v_4 lie on the same line, S_1 degenerates to a 3-flat orthogonal to that line; otherwise it is a 4-dimensional set.⁸ See Fig. 8 for a lower dimensional analog of the situation.

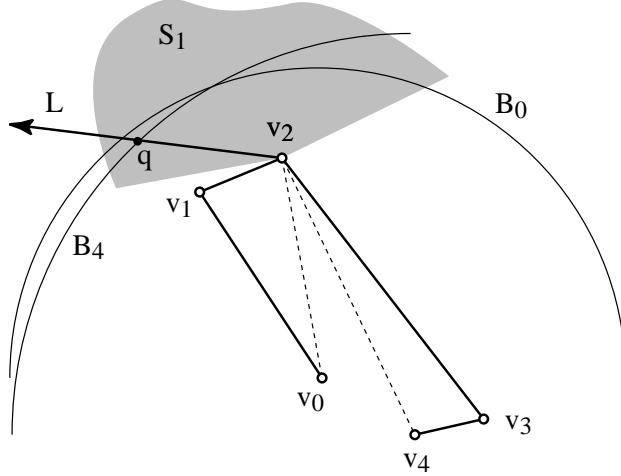


Figure 8: Choosing L . $S_1 \cap S_2 = S_1 \cap (B_0 \cup B_4)$.

The set of points $S_2 = B_0 \cup B_4$ in 4D that satisfy Condition 2 is the union of two 3-spheres, B_0 and B_4 , centered at v_0 and v_4 and of radius r_0 and r_4 , respectively. Because $|v_0v_2| < r_0$ and $|v_2v_4| < r_4$, a neighborhood of v_2 is inside S_2 ; so $S_1 \cap S_2 \neq \emptyset$. The dimensionality of this set depends on whether or not $\{v_0, v_2, v_4\}$ are collinear: if they are, the 3-spheres are intersected by a 3-flat producing 2-spheres; if they are not, the 3-spheres are intersected by a 4-dimensional wedge, producing 3-dimensional regions of the 3-spheres.

Finally, consider Condition 3a; clearly 3b is analogous. We want all those points q such that qv_0 does not intersect any other link of the chain. Clearly

⁸ Although we could remove this possible degeneracy by moving v_2 in a neighborhood (while preserving simplicity) to break the collinearity, this is not necessary, as the proof goes through regardless.

the points forbidden by segment s_i lie in the triangle cone $\Delta_i = \Delta_{v_0}(v_i, v_{i+1})$, just as in the proof of Lemma 8. Intersecting Δ_i for all i with $S_1 \cap S_2$ marks the set of points that must be avoided in our choice of q : $S_3 = \mathbb{R}^4 - \bigcup_i \Delta_i$. It is easiest to concentrate on the intersection of Δ_i with the spheres in S_2 . By Lemma 7, we know this intersection is at most three arcs, independent of the dimension of the spheres. So whether or not $\{v_0, v_2, v_4\}$ are collinear, the intersection produces $O(n)$ arcs. No union of a finite number of 1D arcs can cover the set $S_1 \cap S_2$, which is either 2- or 3-dimensional. Thus $S_1 \cap S_2 \cap S_3 \neq \emptyset$. We need only choose a q in this set.

There are a variety of ways to choose such a q algorithmically. A naive method is to first construct an arrangement of 2D planes in \mathbb{R}^4 , each containing a triangle Δ_i . This computation could be performed in $O(n^4)$ time and space [EOS86] [ESS93]. Intersecting this arrangement with the halfspaces delimiting S_1 and the 3-spheres B_0 and B_4 leave us cells bound by algebraic surfaces inside $S_1 \cap S_2 \cap S_3$. The centroid of any such cell can be selected as q . \square

3.2 Line Tracking in 3D

We start by thinking about the analogous situation in 3D. This will both set notation, and ground intuition by showing why Theorem 5 does not hold in 3D.

3.2.1 Topology of Configuration Space in 3D

Let $\mathbb{R}_{[0,1]}$ be the interval $[0, 1]$ on the real line. We will parametrize the location of v_2 along L by $t \in [0, 1]$, with $t = 0$ the start, and $t = 1$ when v_2 reaches the q of Lemma 12, the first time at which a joint, which we take to be v_1 without loss of generality, straightens. Let \mathcal{C} be the configuration space of the four-link system in isolation, permitting intersections between the links. It should be clear that

$$\mathcal{C} = \mathbb{S}^1 \times \mathbb{S}^1 \times \mathbb{R}_{[0,1]}. \quad (8)$$

This can be seen as follows. Fix some t so that v_2 is fixed. Then each of v_1 and v_3 is free to rotate (independently) on a circle in 3D centered on v_0v_2 and v_2v_4 respectively. As t varies from 0 to 1, these circles move in space, and grow and shrink in radius; see Fig. 9. At $t = 1$ the v_1 circle shrinks to a point. But for $t \in [0, 1)$, both circles retain a positive radius. Thus the configuration space \mathcal{C} has the topology of $\mathbb{S}^1 \times \mathbb{S}^1$ for each t , and the claim follows.

3.2.2 Obstruction Diagram in 3D

As in Section 2, we incorporate the obstacles representing the other links via an “obstruction diagram.” We start by ignoring the four moving links as obstructions, and only consider the remaining, fixed links of the polygonal chain as obstacles. We develop the obstruction diagram first for fixed t , so that the relevant configuration space is $\mathbb{S}^1 \times \mathbb{S}^1$. Because we are ignoring the moving links as obstructions, movement on the two circles is independent, so it suffices

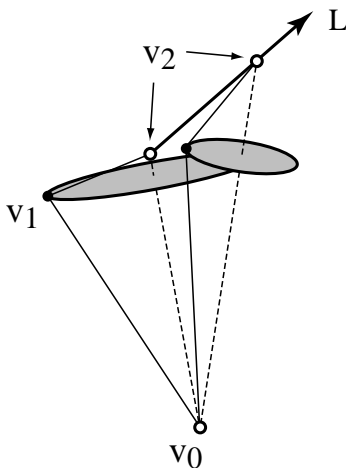


Figure 9: In 3D, the circle on which v_1 may lie moves in space as v_2 slides up L .

to determine the obstruction diagram on one \mathbb{S}^1 , that for v_1 : $\text{Ob}(v_1)$. The following lemma will be key in 4D:

Lemma 13 *In 3D, if $(v_2 - v_0) \cdot (v_1 - v_0) \neq 0$ and $(v_2 - v_0) \cdot (v_1 - v_2) \neq 0$, then a single segment contributes at most four points to $\text{Ob}(v_1)$. Otherwise a segment could obstruct a finite-length arc of the \mathbb{S}^1 circle for v_1 .*

Proof: We only sketch a proof, leaving details for the 4D case considered below. Spinning v_1 along its circle of freedom while maintaining v_0 and v_2 fixed traces out a “spindle” shape, which can be viewed as the union of two cones. A segment s that does not lie along a line through either v_0 or v_2 can intersect each cone in at most two points, and so intersect the spindle in at most four. See Fig. 10. These four segment-cone intersection points correspond one-to-one

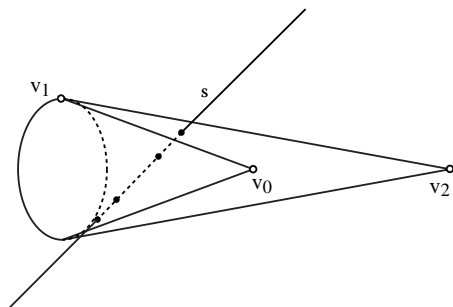


Figure 10: One segment s can contribute four points to $\text{Ob}(v_1)$.

with four v_1 positions on S^1 at which there is an intersection between the 2-link chain (v_0, v_1, v_2) and s .

If the segment s lies in the surface of the cone, then it contributes just one point to the diagram, corresponding to the angle of spin that aligns one of the two links with the obstacle segment.

Finally, if either of the two links v_0v_1 or v_1v_2 is orthogonal to the axis of the spindle, i.e., if either of the dot products in the claim of the lemma is zero, then a segment obstacle could obstruct the entire circle, for one of the cones is degenerately flat. As Fig. 11 illustrates, here a segment might obstruct a range of rotations of $v_2 - v_1$, producing an arc in $\text{Ob}(v_1)$. \square

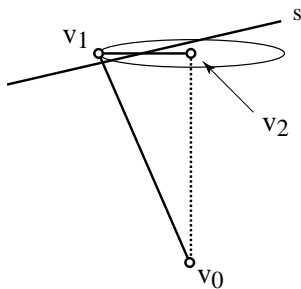


Figure 11: $(v_2 - v_0) \cdot (v_1 - v_2) = 0$ and segment s (which lies in the plane of the circle) contributes an arc to the obstruction diagram $\text{Ob}(v_1)$.

3.2.3 Disconnected Free Space in 3D

Let $v_1(t)$ represent the position of v_1 on its circle S^1 at a particular time t . The goal is for the links (v_0, v_1, v_2) to avoid all obstacles, which means that $v_1(t)$ should avoid points of the obstruction diagram. If we ignore for now the orthogonality case, then we have the situation that a finite set of links produce an obstruction diagram consisting of a finite set of points on S^1 . As t moves, these points wander around the circle, disappear, enter, join, or split. The moving links, previously ignored, just add a few more points to the obstruction diagram, moving in a different manner. The diagram for the full configuration space then looks like arcs on each tube-like copy of $S^1 \times \mathbb{R}_{[0,1]}$. It is clear that it is possible for the point $v_1(t)$ to be “captured” between two points of the obstruction diagram which move together and squeeze $v_1(t)$ into a collision. See Fig. 12. In this case, the *free space* for the point $v_1(t)$ is not connected from $p_1(0)$ to $p_1(1)$. And indeed it is easy to “cage in” the moving links by the fixed links so that no straightening is possible. Our next task is to show that such caging-in is impossible in 4D.

3.3 Line Tracking in 4D

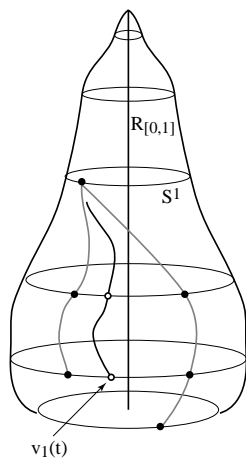


Figure 12: Point $v_1(t)$ is “captured” by two obstacle points in configuration space.

3.3.1 Topology of Configuration Space in 4D

Turning now to 4D, exactly analogous to the situation in 3D, an elbow at the join of two links has a space of possible motions in 4D that is topologically \mathbb{S}^2 , for it is the intersection of two 3-spheres. Thus the configuration space of our four-link chain, ignoring self-intersections, is

$$\mathcal{C} = \mathbb{S}^2 \times \mathbb{S}^2 \times \mathbb{R}_{[0,1]}, \quad (9)$$

where at $t = 1$ at least one of the 2-spheres shrinks to a point.

3.3.2 Obstruction Diagram in 4D

As in 3D, we analyze the obstruction diagram on one \mathbb{S}^2 , that for v_1 , at a fixed value of t : $\text{Ob}(v_1)$. Let $v_1(t)$ represent the position of v_1 on its sphere S^2 at time t . We seek the set of points $\text{Ob}(v_1)$ for which the links (v_0, v_1, v_2) intersect some other segment of the chain, s_4, s_5, \dots, s_n . It may be surprising that, just as in 3D, $\text{Ob}(v_1)$ is (in nondegenerate situations) a finite set of points. This depends on how a line intersects a cone.

Define a $(d-1)$ -cone $C(a, b, \theta)$, for apex point a , axis point b , and cone angle $\theta \in [0, \pi/2]$, to be the set of points $p \in \mathbb{R}^d$ that form an angle θ with respect to the axis, i.e., which satisfy:

$$(p - a) \cdot (b - a) = |p - a| |b - a| \cos \theta. \quad (10)$$

For the extreme values of θ , $C(a, b, 0)$ is a ray from a through b , and $C(a, b, \pi/2)$ is a $(d-1)$ -flat containing a and orthogonal to ab . In 2D, a 1-cone is what we called a triangle cone in Section 2.1.1. In 3D, $C(a, b, \theta)$ is a right circular cone

whose axis is the ray from a through b , and which form the angle θ with the axis at a . Its intersection with a plane orthogonal to ab is a circle. In 4D, $C(a, b, \theta)$ is a “right spherical cone,” whose intersection with a 3D flat orthogonal to ab is a 2-sphere. Note that it is no restriction to insist that $\theta \in [0, \pi/2]$, for we can ensure this for $\theta > \pi/2$ by selecting an axis point b' for the cone to be on the other side of the apex a , on the line containing ab , thereby “reflecting” θ to $\pi - \theta$.

Lemma 14 *The intersection of the $(d-1)$ -cone $C(a, b, \theta)$, $\theta \neq \pi/2$, with a line, ray, or segment whose containing line does not include the apex a , is at most two points: two points, one point, or empty.*

This claim can be seen intuitively as follows. Let C be the cone and s a segment in \mathbb{R}^d . If s is contained in a $(d-1)$ -flat Π orthogonal to ab , then because $\Pi \cap C$ is a sphere, the result follows from Lemma 2. Otherwise s is contained in a flat whose intersection with C is an ellipsoid, and the result follows because an ellipsoid is affinely equivalent to a sphere [Sam88, p. 95]. See Fig. 13.

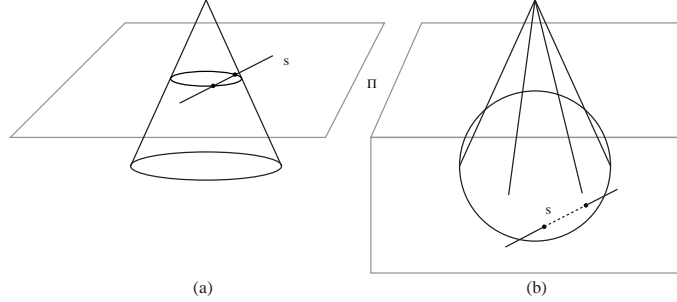


Figure 13: (a) A segment intersects a cone in two points in 3D; (b) A segment intersects a cone in two points in 4D.

Proof: Let $|ab| = 1$ without loss of generality. Translate and rotate C so that $a = (0, 0, \dots, 0)$ and $b = (0, 0, 1, 0, \dots, 0)$. For a point $p = (x_1, \dots, x_d)$, Eq. (10) reduces to

$$p \cdot b = |p| \cos \theta \quad (11)$$

$$(x_1, \dots, x_d) \cdot (0, 0, 1, 0, \dots, 0) = \sqrt{x_1^2 + \dots + x_d^2} \cos \theta \quad (12)$$

$$x_3^2 = (x_1^2 + \dots + x_d^2) \cos^2 \theta \quad (13)$$

Represent the point p via the parameter t :

$$p = (\alpha_1 + \beta_1 t, \dots, \alpha_d + \beta_d t). \quad (14)$$

Substitution of this into Eq. (13) yields a quadratic equation in t , which has at most two roots.

We now examine the degenerate solutions. Because we assumed that $\theta \neq \pi/2$, $\cos \theta \neq 0$. Thus the righthand side of Eq. (13) can only be zero when $x_1^2 + \dots + x_d^2 = 0$, i.e., when $p = (0, 0, \dots, 0)$ is the apex a . This corresponds to a line through a , excluded by our assumptions. \square

Lemma 15 *In 4D, if $(v_2 - v_0) \cdot (v_1 - v_0) \neq 0$ and $(v_2 - v_0) \cdot (v_1 - v_2) \neq 0$, then a single segment s contributes at most four points to $Ob(v_1)$.*

Proof: Moving v_1 sweeps out two finite cones, which are truncations of the infinite cones $C(v_0, v_2, \theta_0)$ and $C(v_2, v_0, \theta_2)$, with

$$(v_2 - v_0) \cdot (v_1 - v_0) = |v_2 - v_0| |v_1 - v_0| \cos \theta_0 \quad (15)$$

$$(v_2 - v_0) \cdot (v_1 - v_2) = |v_2 - v_0| |v_1 - v_2| \cos \theta_2 \quad (16)$$

By the preconditions of the lemma, we have $\theta_j \neq \pi/2$, $j = 0, 2$. We may assume $\theta_j \in [0, \pi/2]$ by the reflection maneuver suggested previously. Consider two cases:

1. The line containing s does not pass through either cone apex, v_0 or v_2 . The conditions of Lemma 14 are satisfied, establishing that s intersects the two cones in at most four points. Each of these points fixes a position of v_1 corresponding to an obstruction, and so contributes this point to $Ob(v_1)$.
2. The line H containing s passes through v_0 (the case through v_2 is exactly analogous and will not be treated separately). Then it may be that $s \cap C(v_0, v_2, \theta_0)$ is a subsegment of s . This is because the vector $p - v_0$ makes the same angle with $v_2 - v_0$ for all $p \in s$ (cf. Eq. (10)). In this case, s obstructs the unique position of v_1 that places it on H , and so contributes just one point to $Ob(v_1)$. Together with the at most two points from the other cone, s generates at most three points of $Ob(v_1)$. \square

The case excluded by the precondition of Lemma 15 refers to the situation in which one cone is degenerately flat, as previously illustrated in Fig. 11. We now analyze this situation in detail.

Lemma 16 *If $(v_2 - v_0) \cdot (v_1 - v_0) = 0$, then $Ob(v_1)$ is a finite set of points and arcs on S^2 .*

Proof: In this case $\theta_0 = \pi/2$ from Eq. (15), and the infinite cone $C(v_0, v_2, \pi/2)$ degenerates to the $(d-1)$ -flat orthogonal to the axis $v_0 v_2$ and including the apex v_0 . The finite cone swept out by the link $s_0 = v_0 v_1$ is a ball B_0 of radius $\ell_0 = |v_0 v_1|$ centered on v_0 . In 3D, B_0 is a disk; in 4D, it is a solid sphere whose boundary is a 2-sphere S^2 representing the possible positions for v_1 .

The positions on S^2 which are obstructed are those for which s_0 intersects some segment s_i . Consider two possibilities:

1. s_i does not lie in the same 3D-subspace of \mathbb{R}^4 as S^2 . Then s_i intersects B_0 in at most one point p (because it can intersect the subspace in at most one point), and then only when s_0 passes through p do we have an obstruction. Thus s_i contributes one point to $Ob(v_1)$.

2. s_i is in the same 3D-subspace of \mathbb{R}^4 as S^2 . Now we have a situation exactly analogous to that shown in Fig. 6: the obstruction is the intersection of the triangle cone $\Delta_{v_0}(v_i, v_{i+1})$ with S^2 . Lemma 3 then establishes that s adds at most two arcs to $\text{Ob}(v_1)$. □

Lemma 17 *The condition $(v_2 - v_0) \cdot (v_1 - v_0) = 0$ can hold at most once (i.e., only at one value of $t \in [0, 1]$) during the movement of v_2 along L .*

Proof: This follows immediately from our choice of L , which guarantees that the distance $|v_0 v_2|$ increases, and so the angle at v_1 opens. This angle can therefore pass through $\pi/2$ at most once. See Fig. 14. □

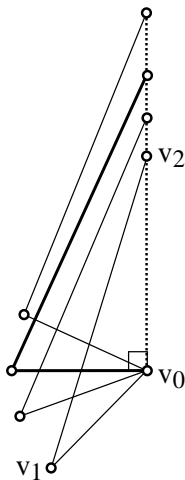


Figure 14: The special condition $(v_2 - v_0) \cdot (v_1 - v_0) = 0$ holds at most once.

3.3.3 Connected Free Space in 4D

Again let $v_1(t)$ represent the position of v_1 on its sphere of possible positions. We first describe the free space for the motion of the 2-link chain (v_0, v_1, v_2) , avoiding the fixed links s_4, s_5, \dots, s_n . It is a subset of $S^2 \times \mathbb{R}_{[0,1]}$. For each $t \in [0, 1]$, we know from Lemma 15 that $\text{Ob}(v_1)$ is a set of points or arcs; and from Lemma 17 we know $\text{Ob}(v_1)$ is a finite set of points, except for at most one t , at which it is a set of points and arcs. Thus if $v_1(t)$ avoids these obstructions, it avoids intersection with the remainder of the chain.

But now it should be clear that it is easy for $v_1(t)$ to “run away” from the obstructions. Think of its sphere of possible positions growing and shrinking with time t . $v_1(t)$ must avoid a set of points at any one time, and once, a set of segments. This is easily done: there is no way to “cage” in $v_1(t)$ with these obstacles. Another view of this situation is that the configuration space

$\mathbb{S}^2 \times \mathbb{R}_{[0,1]}$ is 3-dimensional, and the obstructions $\text{Ob}(v_1(t))$ for $t \in [0, 1]$ are 1-dimensional, and the removal of a 1D set cannot disconnect a 3D set.

We now establish this claim more formally. A *path* in a topological space X is a continuous function $\gamma : [0, 1] \rightarrow X$. A space is *path-connected* if any two of its points can be joined by a path [Arm79]. We first work with the space \mathcal{C}'_1 , where the prime indicates exclusion of $t = 1$.

Lemma 18 *The free space $\mathcal{F}'_1 \subset \mathcal{C}'_1$ for v_1 in the configuration space $\mathcal{C}'_1 = \mathbb{S}^2 \times \mathbb{R}_{[0,1)}$ is path-connected.*

Proof: It will help to view our configuration space as follows. The two-dimensional surface \mathbb{S}^2 is represented by a flat two-dimensional sheet, and $\mathbb{R}_{[0,1)}$ is represented as a vertical axis. The result is a three-dimensional space that could look as depicted in Fig. 15. The point obstacles $\text{Ob}(v_1)$ become paths monotone with respect to the vertical. At one t we may have arc obstacles as well. We need to show that $v_1(0)$ is connected by a path to $v_1(t')$, for any $t' < 1$. We proceed in two cases.

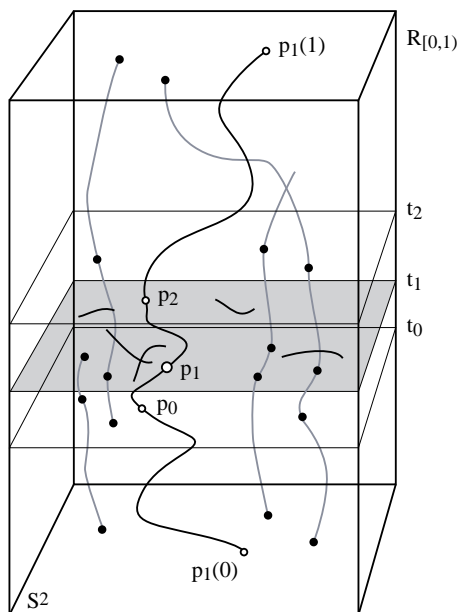


Figure 15: The free space for v_1 is path-connected. The shaded subspace at time $t = t_1$ includes arcs in $\text{Ob}(v_1)$.

1. $\text{Ob}(v_1)$ contains only points for all $t \in [0, 1)$. Let N be the maximum number of points in $\text{Ob}(v_1)$ over all t ; we know $N \leq 2n$. A sphere \mathbb{S}^2 with a finite number N points removed is path-connected. For each t , remove N points from the corresponding \mathbb{S}^2_t : those in $\text{Ob}(v_1)$ at that t , and extra distinct points to “pad out” to N . Any two spheres with the same number

of points removed are homeomorphic. Therefore \mathcal{F}'_1 is homeomorphic to $\mathbb{S}_0^2 \times \mathbb{R}_{[0,1]}$. Because each of those spaces is path-connected, and the product of two path-connected spaces is path-connected, we have established the claim.

2. $\text{Ob}(v_1)$ contains arcs at $t = t_1$. The main idea here is to choose a point $p_1 = v_1(t_1)$ that is unobstructed at time $t = t_1$, and then connect from $v_1(0)$ to p_1 , and from p_1 to $v_1(t')$. It is clear, as we have shown in Case 1, that the spaces $\mathcal{F}_- = \mathcal{C}_{/t \in [0, t_1]}$ and $\mathcal{F}_+ = \mathcal{F}_{/t \in (t_1, 1)}$ are path connected. We will prove that there exist points $p_0 \in \mathcal{F}_-$, and $p_2 \in \mathcal{F}_+$ such that p_0 and p_2 are connected by a path.

We will call a point p *free* if it does not belong to any obstruction diagram. Let $p_1 \in \mathbb{S}_{t_1}^2$ be a free point on $\mathbb{S}_{t_1}^2$. It is clear that such a point exists, since the obstruction diagram is a finite set of arcs and points. It is also clear that there exists a neighborhood $U \subset \mathcal{F}'_1$ of p_1 all of whose points are free. Choose $p_0 \in U$, $p_0 \in \mathbb{S}_{t_0}^2$, $t_0 < t_1$ and $p_2 \in U$, $p_2 \in \mathbb{S}_{t_2}^2$, $t_1 < t_2$. See Fig. 15. Both points are free and can be connected by a path in U to p_1 . But $p_0 \in \mathcal{F}_-$ and $p_2 \in \mathcal{F}_+$, both path connected spaces. Thus we may connect $v_1(0)$ to p_0 to p_1 to p_2 to $v_1(t')$. □

We now address the endpoint $t = 1$. As v_2 approaches q on L , one of the spheres, say that for v_1 , shrinks to zero radius. This is why we restricted our space $\mathbb{R}_{[0,1]}$ to be open at $t = 1$. Thus Fig. 15 is not an accurate depiction near $t = 1$, for the configuration space narrows to a point here.

Lemma 19 *The free space \mathcal{F}_1 for v_1 in the configuration space $\mathcal{C}_1 = \mathbb{S}^2 \times \mathbb{R}_{[0,1]}$ is path-connected.*

Proof: We have chosen q and L in Lemma 12 so that the $t = 1$ endpoint is free in the sense that the straightened chain $v_0v_1v_2$ does not intersect the fixed portion of the chain. Thus there is a neighborhood U of $t = 1$ such that \mathcal{C}_1 is devoid of all obstructions within that neighborhood. Choose $t' \in U$ and apply Lemma 18 to yield a path from $v_1(0)$ to $v_1(t')$. Connect within U from $v_1(t')$ to the endpoint $v_1(1)$. □

So far we have been examining \mathcal{F}_1 , the free space for v_1 avoiding the fixed links s_4, s_5, \dots, s_n .

Lemma 20 *The free space $\mathcal{F} \subset \mathcal{C}$ for both v_1 and v_3 in the configuration space $\mathcal{C} = \mathbb{S}^2 \times \mathbb{S}^2 \times \mathbb{R}_{[0,1]}$ is path-connected.*

Proof: The key here is the independence of the motions of v_1 and v_3 . Let π_1 be a path for $v_1(t)$ through \mathcal{F}_1 , whose existence is guaranteed by Lemmas 18 and 19. Now construct \mathcal{F}_3 as the possible positions $v_3(t)$ for v_3 , avoiding at each time $\text{Ob}(v_3(t))$, where this time the obstructions include not only the fixed links s_4, s_5, \dots, s_n , but also the two moving links s_0 and s_1 , determined by π_1 . If $v_3(t)$ avoids $\text{Ob}(v_3(t))$ for each t , then all intersections are avoided: we do not need to include the moving links in \mathcal{F}_1 , because intersection is symmetric—if the links s_2 and s_3 do not intersect s_0 and s_1 , then s_0 and s_1 do not intersect s_2 and s_3 .

For a fixed t , the obstacles are fixed segments, and $\text{Ob}(v_3)$ is again a finite set of points, or, for at most one t , a set of arcs: Lemmas 15 and 17 apply unchanged. The independence of the motion of v_3 from v_1 permits us to treat the moving segments s_0 and s_1 on par with the fixed segments: the only difference is that their obstacle points move through $\mathcal{C}_3 = \mathbb{S}^2 \times \mathbb{R}_{[0,1]}$ differently. Therefore a path π_3 for $v_3(t)$ may be found in $\mathcal{F}_3 \subset \mathcal{C}_3$. The two paths π_1 and π_3 , together with the ray L for v_2 , constitute a path for moving the 4-link chain $(v_0, v_1, v_2, v_3, v_4)$ while maintaining simplicity. \square

This finally completes the proof of Theorem 5.

3.4 Motion Planning

We now know a path that avoids self-intersection exists, i.e., either the joint v_1 or v_3 can be straightened. The next step is to compute such a path algorithmically. We rely on general motion planning algorithms, as in Section 2.1.3.

Our “robot” consists of the four links $(v_0, v_1, v_2, v_3, v_4)$ moving in the 5-dimensional configuration space \mathcal{C} , Eq. (9). The subspace \mathcal{C}_0 that avoids self-intersection between the four links is some semialgebraic subset of \mathcal{C} , semialgebraic because the constraints on self-intersection may be written in Tarski sentences (see, e.g., [Mis97]). The free configuration space \mathcal{F} is composed of the points of \mathcal{C}_0 that avoid the obstacles, which is again a semialgebraic set. Canny’s Roadmap algorithm achieves a time and space complexity of $O(n^5 \log n)$, where n is the number of obstacles, because in our case, the configuration space has $k = 5$ dimensions. The algorithm produces a piecewise algebraic path through \mathcal{F} , of $O(n^5)$ pieces. Each piece constitutes a constant number of moves, and so each joint straightening can be accomplished in $O(n^5)$ moves. Repeating the planning and straightening n times leads to $O(n^6)$ moves in $O(n^6 \log n)$ time. Because choosing L times requires at most $O(n^4)$ time by Lemma 12, the time complexity is dominated by the path planning, thereby establishing the bounds claimed in Theorem 2.

4 Higher Dimensions

We have already shown that every simple open/closed chain in 4D can be straightened/convexified. Our final task is to prove that this result holds for higher dimensions, using the results from 4D.

For an open chain, we straighten four links at a time and then repeat the procedure until the chain is straight. If the chain contains less than four links, then it determines a space that has at most dimension three, and it can be included in a 4D-space. For a closed chain, our algorithm also moves four links at a time. Four links determine a space that is at most 4-dimensional, which means that it can be included in a 4D-subspace of our d -dimensional space \mathbb{R}^d , $d \geq 4$.

We have already shown that these four links, for both open and closed chains, can be straightened in 4D; therefore, they can be straightened in this

4D-subspace of \mathbb{R}^d . We only have to worry about the pieces of the remainder of the chain that intersect this 4D-subspace. But since we are dealing with segments, their intersection with a 4D-subspace is either a point or a segment. But these are the kind of obstructions we have proven that can be avoided in 4D. Therefore, the straightening of these four links can be completed in the 4D-subspace, and therefore in the d -dimensional space \mathbb{R}^d , while maintaining rigidity and simplicity.

The complexity for the algorithms in d -dimensional spaces, $d \geq 4$, is the same as for the algorithms in 4D, for all computations are performed in 4D subspaces. This proves Theorem 3.

Acknowledgement. We thank Erik Demaine for helpful comments, and Godfried Toussaint for the Sallee reference [Sal73].

References

- [Ada94] C. C. Adams. *The Knot Book*. W. H. Freeman, New York, 1994.
- [Arm79] M. A. Armstrong. *Basic Topology*. McGraw-Hill, London, UK, 1979.
- [BDD⁺99] T. Biedl, E. Demaine, M. Demaine, S. Lazard, A. Lubiw, J. O’Rourke, M. Overmars, S. Robbins, I. Streinu, G. Toussaint, and S. Whitesides. Locked and unlocked polygonal chains in 3D. In *Proc. 10th ACM-SIAM Sympos. Discrete Algorithms*, pages 866–867, January 1999.
- [CF65] R. H. Crowell and R. H. Fox. *Introduction to Knot Theory*. Blaisdell Publishing Co., New York, NY, 1965.
- [CJ98] J. Cantarella and H. Johnston. Nontrivial embeddings of polygonal intervals and unknots in 3-space. *J. Knot Theory Ramifications*, 7:1027–1039, 1998.
- [Coc99] R. Cocan. Polygonal chains cannot lock in 4D. Undergraduate thesis, Smith College, April, 1999.
- [EGP⁺92] H. Edelsbrunner, Leonidas J. Guibas, J. Pach, R. Pollack, R. Seidel, and Micha Sharir. Arrangements of curves in the plane: Topology, combinatorics, and algorithms. *Theoret. Comput. Sci.*, 92:319–336, 1992.
- [ELR⁺98] H. Everett, S. Lazard, S. Robbins, H. Schröder, and S. Whitesides. Convexifying star-shaped polygons. In *Proc. 10th Canad. Conf. Comput. Geom.*, pages 2–3, 1998.
- [EOS86] H. Edelsbrunner, J. O’Rourke, and R. Seidel. Constructing arrangements of lines and hyperplanes with applications. *SIAM J. Comput.*, 15:341–363, 1986.
- [ESS93] H. Edelsbrunner, R. Seidel, and Micha Sharir. On the zone theorem for hyperplane arrangements. *SIAM J. Comput.*, 22(2):418–429, 1993.
- [Hal97] D. Halperin. Arrangements. In Jacob E. Goodman and Joseph O’Rourke, editors, *Handbook of Discrete and Computational Geometry*, chapter 21, pages 389–412. CRC Press LLC, Boca Raton, FL, 1997.
- [HY61] J. G. Hocking and G. S. Young. *Topology*. Addison-Wesley, Reading, MA, 1961.
- [LW95] W. J. Lenhart and S. H. Whitesides. Reconfiguring closed polygonal chains in Euclidean d -space. *Discrete Comput. Geom.*, 13:123–140, 1995.

- [Mis97] B. Mishra. Computational real algebraic geometry. In Jacob E. Goodman and Joseph O'Rourke, editors, *Handbook of Discrete and Computational Geometry*, chapter 29, pages 537–558. CRC Press LLC, Boca Raton, FL, 1997.
- [Sal73] G. T. Sallee. Stretching chords of space curves. *Geometriae Dedicata*, 2:311–315, 1973.
- [Sam88] P. Samuel. *Projective Geometry*. Springer-Verlag, 1988.
- [Sha97] M. Sharir. Algorithmic motion planning. In Jacob E. Goodman and Joseph O'Rourke, editors, *Handbook of Discrete and Computational Geometry*, chapter 40, pages 733–754. CRC Press LLC, Boca Raton, FL, 1997.
- [Thu97] W. Thurston. *Three-Dimensional Geometry and Topology, Volume 1*. Princeton Univ. Press, 1997.
- [Tou99] G. T. Toussaint. A new class of stuck unknots in Pol_6 . Technical Report SOCS-99.1, School of Comput. Sci., McGill Univ., 1999.